Sodium (^{23}Na)-Imaging as Therapy Monitoring in Oncology – Future Prospects

Stefan Haneder, M.D.[1]; Stefan O. Schoenberg, M.D.[1]; Simon Konstandin, Ph.D.[2]; Lothar R. Schad, Ph.D.[2]

[1]*Institute of Clinical Radiology and Nuclear Medicine, University Medical Center Mannheim, Heidelberg University, Mannheim, Germany*
[2]*Computer-Assisted Clinical Medicine, Heidelberg University, Mannheim, Germany*

Introduction

"Form follows function" – Louis Sullivan, 1896

Whilst this concept was originally applied to modern architecture, it could well become a highly appropriate maxim for future imaging and therapy concepts. Magnetic resonance imaging (MRI) has continually developed into a powerful, widely used diagnostic tool and offers the opportunity to expand traditional imaging concepts based on morphological information. In the future, the pure morphology will remain a central component of multimodal imaging, but will be flanked increasingly by functional approaches reaching far beyond the current imaging standards. In oncological therapy follow-up the drawback of relying on pure morphology is widely known, resulting, for example, from delayed morphological reflection of tumor regression. Consequently, the RECIST Working Group addressed this point in the context of the new RECIST1.1 criteria [1]:

„A key question considered by the RECIST Working Group in developing RECIST 1.1 was whether it was appropriate to move from anatomic unidimensional assessment of tumour burden to either volumetric anatomical assessment or to **functional assessment with PET or MRI**. It was concluded that, at present, there is not sufficient standardisation or evidence to abandon anatomical assessment of tumour burden. The only exception to this is in the use of FDG-PET imaging as an adjunct to determination of progression. [...]"

This statement contains several basic implications for future MR strategies of therapy control. **First**, the internal radiology benchmark of functional MR sequences seems to be nuclear medicine approaches, already fixed in guidelines as PERCIST 1.0 [2]. **Second**, further multicenter, international studies are required to obtain reliable data for (functional) MR approaches. **Third** – not explicitly, but indirectly – the radiology community should not abandon the assessment of new functional approaches and should try to implement them in clinical settings. The arsenal of current functional MR imaging approaches includes diffusion-weighted imaging (DWI), diffusion tensor imaging (DTI), arterial spin labeling (ASL), blood-oxygenation level dependent imaging (BOLD) and sodium (^{23}Na)-imaging. DWI [3] should be emphasized as a kind of paradigm shifting technique. Since the 1990s DWI has been performed for intracranial diseases and has contrib-

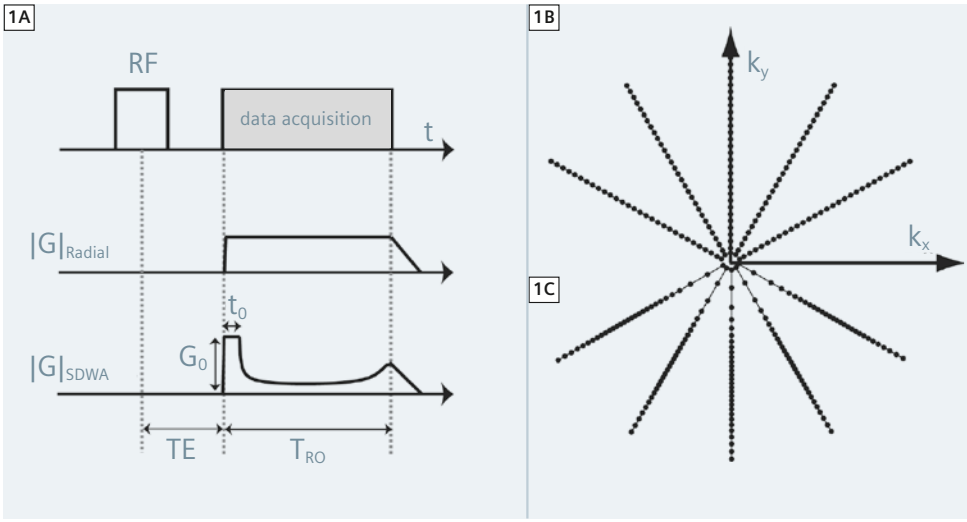

1 Sequence design for 3D radial acquisition with global excitation. Absolute gradient values ($\sqrt{G_x^2+G_y^2+G_z^2}$) are shown for standard radial acquisition with constant gradient readout ($|G|_{Radial}$) and sampling density-weighted apodization ($|G|_{SDWA}$) for intrinsic filtering. Due to hardware restrictions the gradient adaption begins at $t = t_0$ with gradient amplitude G_0. The echo time TE is defined as the time interval between the middle of the RF pulse and the beginning of data acquisition with readout duration T_{RO}. The *k*-space sample points are exemplarily shown in the k_{xy}-plane for standard radial **(1B)** and SDWA **(1C)** acquisition. *Figure adapted from [18].*

uted to the detection of early stroke. But in recent years the number of studies has increased substantially, evaluating this method in detection and characterization of lesions, especially in the field of oncology and the possibility of (early) tumor treatment response [4-8]. This remarkable success story cannot (yet) be applied to ^{23}Na imaging, but we are witnessing continuous development.

Physiological and technical basics

^{23}Na ions play a fundamental role in human life and can be traced – similar to protons (^{1}H) – ubiquitary in the human body. Fluxes of ^{23}Na ions in cells and across cell membranes are central part of many processes of cell activity. Up to 70% of the energy from adenosine triphosphate (ATP) hydrolysis is used for the Na^+-K^+-ATPase, which pumps three Na^+ ions out of the cell while two K^+ ions vice versa [9]. An extracellular concentration of ≈145 mM and an intracellular concentration of ≈12–20 mM (10) are maintained in healthy tissue by this pump mechanism, which leads to a mean tissue sodium concentration (TSC) of about 50 mM. Pathologic changes such as tissue injury, edema, or necrosis result in a degradation of Na^+-K^+-ATPase and hence in an increase in TSC from 50 mM up to 145 mM in case of cell burst [11].

From an electro-physiological point-of-view, some physical characteristics of ^{23}Na hamper the simple application for MR imaging. The sodium nucleus has a spin of 3/2 and is therefore subject to quadrupolar relaxation resulting in a biexponential T2 decay with relaxation times of T2f* 0.5-8 ms and T2s* 15–30 ms for the fast and slow component, respectively [12]. Additionally, sodium MRI suffers from low *in vivo* concentration with a weak gyromagnetic ratio of only ¼ of that for ^{1}H resulting in an approximately 10-fold lower MR sensitivity compared to ^{1}H MRI with about 10,000-fold less signal. Consequently, signal-to-noise ratio (SNR)-efficient acquisition strategies with short echo times such as the radial scheme [13] are required. Many MR sequences were recently developed to acquire the k-space homogeneously yielding higher SNR: twisted projection imaging (TPI) [14], 3D cones [15], density-adapted projection reconstruction [16, 17]. Since filtering is usually applied to sodium images as a post-processing step, sampling density-weighted apodization (SDWA) with intrinsic filtering [18, 19] is preferred when using short readout durations (Fig. 1). Anisotropic 3D imaging sequences using cones [20] or twisted projection imaging [21] were recently developed for applications where anisotropic resolutions are needed (e.g., cartilage).

The technical developments of acquisition strategies and sequence design over the last decade were accompanied by MR hardware improvements. The trend to higher field strengths and stronger gradient systems was continued and led not only to a routine use of 3T MR scanners in patient care but to a growing number of 7T whole-body-MR installations worldwide. The electro-physiological characteristics of ^{23}Na predestine the implementation of higher field strengths. Complementary progression can be stated for coil design. Meanwhile multi-channel ^{23}Na coils are commercially available and experimental new designs – as a double-tuned two-port surface resonator for ^{23}Na- and ^{1}H-imaging [22, 23] – have been introduced.

Oncologic therapy monitoring using ^{23}Na MRI – quo vadis?

Taking into account the above-described technical developments over the last few years, a kind of renaissance of ^{23}Na-MRI and the determination of tissue sodium content (TSC) can be stated. Feasibility of ^{23}Na-MRI for *in vivo* imaging of physiological conditions has been demonstrated in various parts of the human body, e.g. kidney [24-26], cartilage and musculoskeletal in general [12, 27-29], brain [30, 31] heart [32-34] and prostate [35]. Initial translation from physiology to pathophysiology was correspondingly addressed in a broad spectrum of organs and different pathologies. The possibility of imaging of transplanted kidneys [36] and detection of renal changes after 3 dimensional conformal radiotherapy in a long-term follow-up in patients after gastric cancer [37], has been shown. In musculoskeletal imaging, for example, different cartilage repair approaches in the knee were evaluated with ^{23}Na-MRI at 7T [38-40] and presented marked differences in comparison to native cartilage.

Increased sodium concentrations were found in different brain tumors relative to normal brain structures [41, 42]. An up to threefold increase in TSC can be observed in human stroke [43] allowing monitoring of the progression of stroke pathophysiology [44, 45]. Surprising results revealed a study about relapsing-remitting multiple sclerosis at early and advanced stage. TSC was increased inside demyelinating lesions in both groups of patients, but TSC accumulation dramatically increases in the advanced stage, especially in the normal-appearing brain tissues, concomitant with disability [46]. Furthermore, ^{23}Na-MRI provides a non-invasive solution to distinguish viable from nonviable myocardial tissue after myocardial infarction in an animal model [47] and in humans [48, 49]. TSC measurements have shown an increased signal mainly in nonviable myocardium after infarction due to loss of cell membrane integrity. Despite the never-ending discussion of necessity of separating intra- and extracellular ^{23}Na components, TSC offers a unique tool for measuring tissue viability noninvasively. The pathophysiology phenomena in almost all acute pathologies (stroke, myocardial infarction) are mainly based on the idea of changing ^{23}Na environments e.g. due to the loss of cell membrane integrity and the following adjustment of intra- and extracellular ^{23}Na concentrations. Laymon et al. [50] described that cell membrane depolarization preceding the large degree of cell division in neoplastic tissue leads to an increase in the intracellular sodium concentration (ISC) and a concomitant rise in the total TSC. In human brain tumors, Ouwerkerk and co-workers showed that measured ^{23}Na changes within the tumors cannot only be attributed to alterations in ^{23}Na relaxation time, e.g. in the presence of surrounding edema, but reflect

real intrinsic changes of Na^+-K^+-pump function [41]. This research group concluded in the same work as prospect to therapy monitoring:
"Therapies that alter tumor ion homeostasis or affect or destroy tumor cell membrane integrity are likely to generate changes that are observable with ^{23}Na MR imaging and sodium concentration measurements. With these measurements, changes can be observed much earlier than the effects of anatomic remodeling."
This idea of using ^{23}Na as surrogate parameter for oncology therapy control is therefore not new and was among others also addressed by Thulborn et al. [42] in the field of management of brain tumors. The ability to quantify early effects of tumor therapeutic response using non-invasive ^{23}Na-MR imaging approaches would have a major impact in clinical oncology. To date, clinical studies assessing these predicted potentials are missing, but first data, mainly derived from different animal models, apart from several tumor entities, have been published.
In 2000, Kline et al. [51] detected significantly increased ^{23}Na signal in mouse xenograft tumors propagated from human prostate cancer cell lines, 24h after administration of antineoplastics compared to baseline. Histopathological correlation of explanted tumors confirmed that chemotherapy reduced proliferation, inversely correlated with ^{23}Na MRI response on a tumor-to-tumor basis. A logical development was the combination with another functional MR approach. Babsky et al. [52] performed ^{23}Na-MRI and DWI in a mice model with subcutaneously-implanted radiation-induced fibrosarcoma (RIF-1) before, and daily for 3 days after, chemotherapy treatment. In contrast to the control group, *in vivo* MRI experiments showed an increase in both ^{23}Na and apparent diffusion coefficient (ADC) in treated tumors, correlating to histological confirmed decreased cell density. After chemotherapy a chemical analysis showed an increased relative extracellular space and [Na^+] concentration in treated tumors. Sharma and co-workers [53] evaluated at 4.23T the association between *in vivo* intracellular ^{23}Na MRI intensities, immuno-biomarkers and histopathological features respectively, to monitor the early tumor response to chemotherapy using a rat xenograft breast tumor model. They concluded that intracellular ^{23}Na MRI intensities possibly indicate chemosensitivity response *in vivo* associated with apoptosis and different pre-malignant features within 24 hours of exposure of cancer cells to anti-neoplastic Taxotere drug.
Schepkin et al. [54] compared ^{23}Na and DWI for their ability to detect early cellular changes in rats with subcutaneous 9L gliosarcomas treated with chemotherapy. Both imaging modalities were able to detect early changes (2 days post-treatment) in tumor cellularity continuing to evolve to a maximum after 8 days. Subsequent tumor shrinkage followed the functional parameters. The authors concluded that therapeutically-induced changes in ^{23}Na and DWI were found to have similar dynamic and spatial changes and detect similar early cellular changes after treatment. The same research group demonstrated the sensitivity and applicability of ^{23}Na and DWI as tools for dynamic assessment of tumor response to therapy [55]. They detected in a 9L rat gliosarcoma model, a correlation between tumor ^{23}Na and DWI to gauge tumor response to therapy with varying doses of chemotherapy.
In summary, all animal studies confirmed the possibility to detect tumor changes with ^{23}Na imaging after oncologic therapy as correlation of treatment success. But the really astonishing finding of these preclinical studies is the indication that ^{23}Na MRI could develop into an early predictor of therapy response within the first 24h. If these results were to be affirmed in human studies, it could lead to a major medical

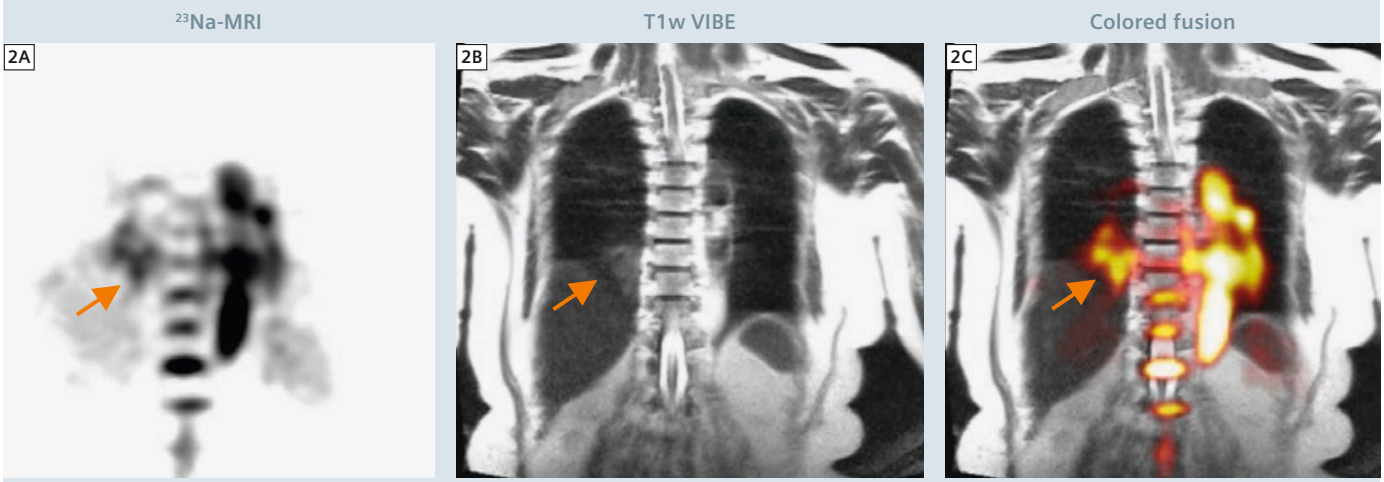

2 Image examples, including **(2A)** ^{23}Na-MRI, **(2B)** morphological T2w HASTE (Half fourier-Acquired Single shot Turbo spin Echo) and **(2C)** a colored fusion of both sequences, of a 66-year-old male patient with lung cancer (stage IV adenocarcinoma). The lung cancer in the right lower lobe is marked with an arrow. *Courtesy of PD Dr. Thomas Henzler, University Medical Center Mannheim, Heidelberg University, Germany*

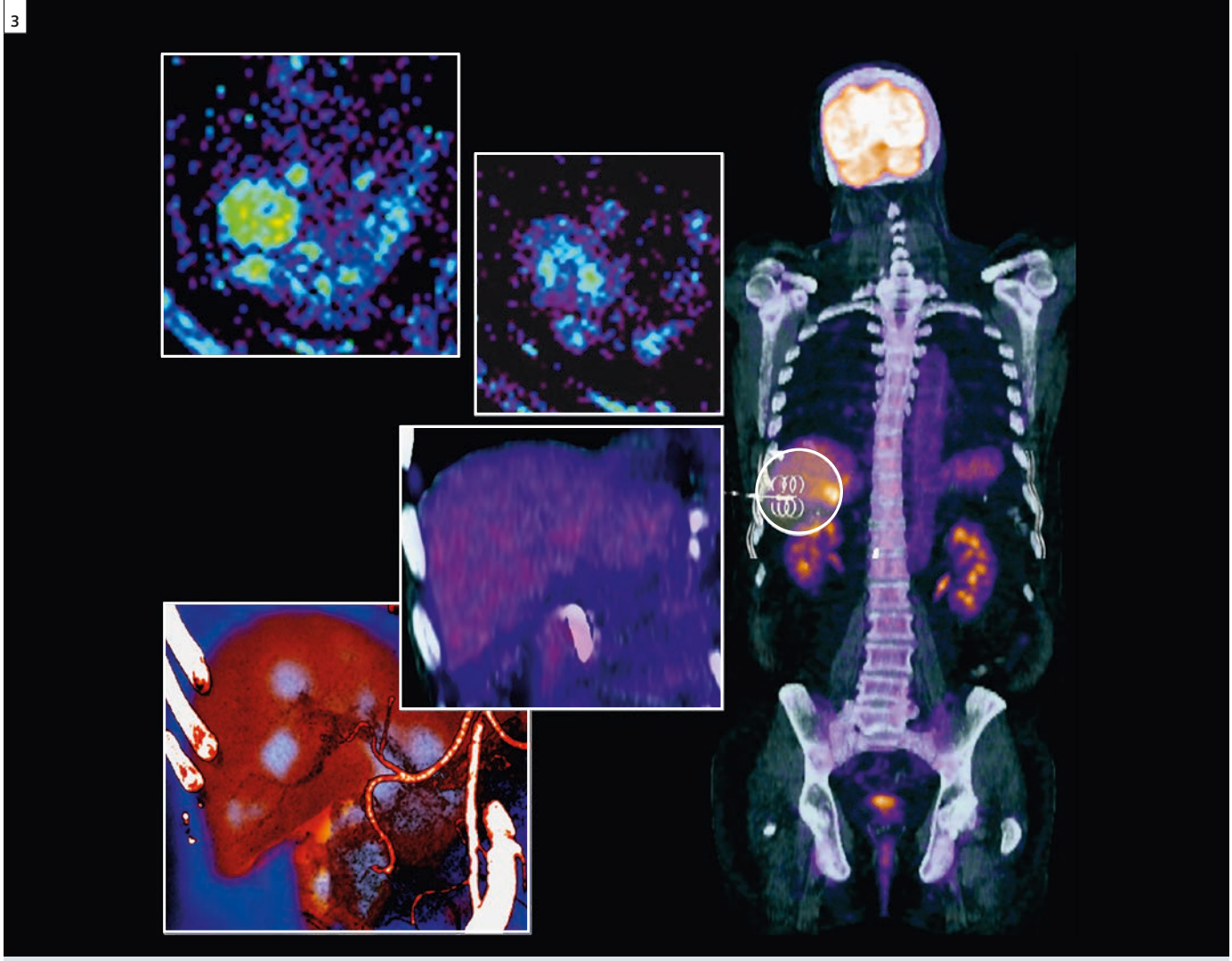

3 Potential multimodal treatment planning combining different currently available functional approaches such as DWI and ^{18}F-FDG-PET-CT supporting the need for further MRI techniques such as ^{23}Na-MRI [59].

and economical impact on oncological therapy control and generate an early imaging tool for personalized therapy control.

One of the first *in vivo* translation into human pathologies in oncology treatment monitoring was reported by Henzler et al. [56], who showed the feasibility of ^{23}Na-MRI in patients with lung cancer (Fig. 2). In this feasibility study, three patients with stage IV adenocarcinoma of the lung were enrolled and multimodal examined. Data were available of ^{23}Na- and non-contrast enhanced ^{1}H-MRI, CT and ^{18}F-FDG-PET-CT. One of the three included patients was chemonaive and examined before and after the initiation of combination therapy. Fusion of ^{23}Na-MR images with ^{1}H-MRI, CT and FDG-PET-CT was feasible in all patients and showed differences in solid and necrotic tumor areas. Between the two exams the signal intensity of the tumor as well as the ratio of signal intensity between the tumor and the CSF slightly increased indicating early therapy induced changes within the tumor. The authors concluded that ^{23}Na-MRI is feasible in patients with lung cancer and could provide valuable functional molecular information regarding tumor viability, and potentially a treatment response.

A second example was recently published by Layman et al. [50] from the University of Pittsburgh. This research group aimed in their feasibility study to implement and compare [^{18}F]-fluorothymidine (^{18}F-FLT) positron emission tomography (PET), ^{23}Na and morphological MRI at 3T in patients with glioblastoma multiforme. Two patients underwent repetitive scans at baseline (before therapy), at an early and a late follow-up time point after beginning therapy. Both functional methods were registered to the morphological MRI and calculated on a voxel-wise basis to address the heterogeneity of tumor physiology. Both – ^{18}F-FLT PET and ^{23}Na-MRI – independently presented changes of the tumor tissue varying in different regions, as a function of scan time point. But these initial results indicate that the two functional modalities may provide complementary information regarding tumor progression and response. The authors stated that, unlike ^{18}F-FLT uptake, changes in sodium concentration occur without limitations from the state of the blood brain barrier. But the final value of ^{23}Na MRI in these patients and the possibility to discriminate tumor progression from pseudoprogression requires additional patient data and outcome control. Undoubted ^{23}Na MRI is an auspicious

functional technique, for which the preclinical animal and first *in vivo* human data show a huge potential in the field of oncology treatment. However, this technique clearly still requires a special and sophisticated technical setup, which up to now is only available in a select number of research centers worldwide.

Integrated concepts of functional therapy +/– monitoring*

The great challenge for the coming years is to translate this additional diagnostic information into a more effective, less invasive therapy for the patient with fewer side effects and at the same time higher cost-effectiveness rendering it more affordable for the general health care system. This implies that imaging is specific for the mechanism of the disease and the target of the therapy on one hand and provides a complete picture of the systemic spread and thus the stage of the disease on the other. For this, the critical gap between modern molecular histopathology, molecular imaging and image-guided, minimally-invasive therapy has to be bridged and the results transferred from basic science into clinical routine. This challenge cannot be comprehensively addressed by a single research group, but requires the close interaction of scientists from multiple disciplines of medical imaging and from different types of academic institutions as well as industry in close proximity on a medical university campus. Currently, industry on campus (IOC) initiatives such as the one from the German Federal Ministry of Research in Germany are specifically designed to facilitate this type of interdisciplinary, patient-focused research on a single campus in a long-term private-public partnership. As an example, the initiative 'Mannheim Molecular Intervention Environment (M^2OLIE)' aims at developing a closed-loop treatment process in oligometastatic patients spanning from personalized molecular imaging to target-specific minimally-invasive multimodal therapy. Patients with a previously treated oncologic disease and de novo development of a few metastases are the fastest growing group of cancer patients. With dedicated multimodal minimally-invasive therapies a stabilization of the disease can be potentially achieved with survival times almost similar to those in cured patients. The key to a precise elimination of these metastases is the detailed tumor characterization, as current studies have shown that the individual tumor cell clones of each lesion substantially differ from each other [57].

The key to a successful implementation of these techniques is the seamless integration of the entire diagnostic information into a single comprehensive therapeutic modality. Within the last 5 years substantial innovations have been brought into clinical routine by a close cooperation between industry, scientists and clinicians: state-of-the art robot-assisted X-ray systems offer much higher degrees of freedom for placement of needles and catheters and at the same time allow for image-guided control of the intervention by use of rotating flat panels. New algorithms for dose reduction such as compressed sensing will enable time-resolved 4D imaging with a fraction of currently applied radiation doses [58]. New molecular contrast mechanisms in MRI such as ^{23}Na imaging, as described above, could play a key role in this comprehensive setting since images from 4D CT, functional MRI and PET data can be fused using current advances in software and provide information for the interventionist on blood flow and metabolism of the tumor in real-time (Fig. 3).

*Adapted from [59].

Conclusion

Taking into account the three basic implications deduced in the introduction, ^{23}Na-MRI undeniably has still a long way to go. But – also undeniably – ^{23}Na-MRI clearly shows promise as an outstanding new approach for measuring tissue viability non-invasively. And its full potential is by no means exhausted. This technique can develop into a non-invasive avenue of therapy monitoring for a variety of diseases, particularly, but not solely, in oncological settings.

Acknowledgment

We thank PD Dr. Thomas Henzler, University Medical Center Mannheim, Heidelberg University for providing Figure 2.

References

1 Eisenhauer EA, Therasse P, Bogaerts J, et al. New response evaluation criteria in solid tumours: revised RECIST guideline (version 1.1). Eur J Cancer. 2009;45(2):228-47.
2 Wahl RL, Jacene H, Kasamon Y, Lodge MA. From RECIST to PERCIST: Evolving Considerations for PET response criteria in solid tumors. J Nucl Med. 2009;50 Suppl 1:122S-50S.
3 Le Bihan D, Breton E, Lallemand D, Aubin ML, Vignaud J, Laval-Jeantet M. Separation of diffusion and perfusion in intravoxel incoherent motion MR imaging. Radiology. 1988;168(2): 497-505.
4 Koh DM, Collins DJ. Diffusion-weighted MRI in the body: applications and challenges in oncology. AJR American journal of roentgenology. 2007;188(6):1622-35.
5 Taouli B, Koh DM. Diffusion-weighted MR imaging of the liver. Radiology. 2010;254(1):47-66.
6 Desouza NM, Reinsberg SA, Scurr ED, Brewster JM, Payne GS. Magnetic resonance imaging in prostate cancer: the value of apparent diffusion coefficients for identifying malignant nodules. Br J Radiol. 2007;80(950):90-5.
7 Sinha S, Lucas-Quesada FA, Sinha U, DeBruhl N, Bassett LW. In vivo diffusion-weighted MRI of the breast: potential for lesion characterization. Journal of magnetic resonance imaging : JMRI. 2002;15(6):693-704.
8 Kwee TC, Takahara T, Ochiai R, et al. Whole-body diffusion-weighted magnetic resonance imaging. European journal of radiology. 2009;70(3): 409-17.
9 Silbernagl S, Despopoulos A. Color Atlas of Physiology. New York.: Thieme, 2003.
10 Hilal S, Ra J, Oh C, Mun I, Einstein S, Roschmann P. Sodium imaging. . In: Stark D, Bradly W, eds. Magnetic resonance imaging. St. Louis 1988; p. 715–29.
11 Boada FE, LaVerde G, Jungreis C, Nemoto E, Tanase C, Hancu I. Loss of cell ion homeostasis and cell viability in the brain: what sodium MRI can tell us. Curr Top Dev Biol. 2005;70:77-101.
12 Constantinides CD, Gillen JS, Boada FE, Pomper MG, Bottomley PA. Human skeletal muscle: sodium MR imaging and quantification-potential applications in exercise and disease. Radiology. 2000;216(2):559-68.
13 Lauterbur P. Image formation by induced local interactions: examples employing nuclear magnetic resonance. Nature. 1973;242(5394):190–1.
14 Boada FE, Shen GX, Chang SY, Thulborn KR. Spectrally weighted twisted projection imaging: reducing T2 signal attenuation effects in fast three-dimensional sodium imaging. Magn Reson Med. 1997;38(6):1022-8.
15 Gurney PT, Hargreaves BA, Nishimura DG. Design and analysis of a practical 3D cones trajectory. Magn Reson Med. 2006;55(3):575-82.
16 Nagel AM, Laun FB, Weber MA, Matthies C, Semmler W, Schad LR. Sodium MRI using a

density-adapted 3D radial acquisition technique. Magn Reson Med. 2009;62(6):1565-73.
17 Konstandin S, Nagel AM, Heiler PM, Schad LR. Two-dimensional radial acquisition technique with density adaption in sodium MRI. Magn Reson Med. 2011;65()4;1090-6.
18 Konstandin S, Nagel AM. Performance of sampling density-weighted and postfiltered density-adapted projection reconstruction in sodium magnetic resonance imaging. Magn Reson Med. 2013;69(2):495-502.
19 Stobbe R, Beaulieu C. Advantage of sampling density weighted apodization over postacquisition filtering apodization for sodium MRI of the human brain. Magn Reson Med. 008;60(4):981-6.
20 Staroswiecki E, Bangerter NK, Gurney PT, Grafendorfer T, Gold GE, Hargreaves BA. In vivo sodium imaging of human patellar cartilage with a 3D cones sequence at 3 T and 7 T. Journal of magnetic resonance imaging : JMRI. 2010;32(2):446-51.
21 Watts A, Stobbe RW, Beaulieu C. Signal-to-noise optimization for sodium MRI of the human knee at 4.7 Tesla using steady state. Magn Reson Med. 2011;66(3):697-705.
22 Wetterling F, Hogler M, Molkenthin U, et al. The design of a double-tuned two-port surface resonator and its application to in vivo hydrogen- and sodium-MRI. J Magn Reson. 2012;217:10-8.
23 Wetterling F, Corteville DM, Kalayciyan R, et al. Whole body sodium MRI at 3T using an asymmetric birdcage resonator and short echo time sequence: first images of a male volunteer. Phys Med Biol. 2012;57(14):4555-67.
24 Haneder S, Konstandin S, Morelli JN, et al. Quantitative and Qualitative 23Na MR Imaging of the Human Kidneys at 3 T: Before and after a Water Load. Radiology. 2011;260(3):857-65.
25 Maril N, Rosen Y, Reynolds GH, Ivanishev A, Ngo L, Lenkinski RE. Sodium MRI of the human kidney at 3 Tesla. Magn Reson Med. 2006;56(6):1229-34.
26 Haneder S, Kettnaker P, Konstandin S, et al. Quantitative in vivo 23Na MR-Imaging of the healthy human kidney: determination of physiological ranges at 3.0T with comparison to DWI and BOLD. Magma. 2013: in press; DOI 10.1007/s10334-013-0369-4.
27 Trattnig S, Zbyn S, Schmitt B, et al. Advanced MR methods at ultra-high field (7 Tesla) for clinical musculoskeletal applications. European radiology. 2012;22(11):2338-46.
28 Noebauer-Huhmann IM, Juras V, Pfirrmann CW, et al. Sodium Imaging of the Lumbar Intervertebral Disk at 7 T: Correlation with T2 Mapping and Modified Pfirrmann Score at 3 T – Preliminary Results. Radiology. 2012.
29 Borthakur A, Shapiro EM, Akella SV, Gougoutas A, Kneeland JB, Reddy R. Quantifying sodium in the human wrist in vivo by using MR imaging. Radiology. 2002;224(2):598-602.
30 Clayton DB, Lenkinski RE. MR imaging of sodium in the human brain with a fast three-dimensional gradient-recalled-echo sequence at 4 T. Acad Radiol. 2003;10(4):358-65.
31 Kohler S, Preibisch C, Nittka M, Haase A. Fast three-dimensional sodium imaging of human brain. Magma. 2001;13(2):63-9.
32 Jerecic R, Bock M, Nielles-Vallespin S, Wacker C, Bauer W, Schad LR. ECG-gated 23Na-MRI of the human heart using a 3D-radial projection technique with ultra-short echo times. Magma. 2004;16(6):297-302.
33 Konstandin S, Schad LR. Two-dimensional radial sodium heart MRI using variable-rate selective excitation and retrospective electrocardiogram gating with golden angle increments. Magn Reson Med. 2012. doi: 10.1002/mrm.24523
34 Greiser A, Haase A, von Kienlin M. Improved cardiac sodium MR imaging by density-weighted phase-encoding. Journal of magnetic resonance imaging : JMRI. 2005;21(1):78-81.
35 Hausmann D, Konstandin S, Wetterling F, et al. Apparent Diffusion Coefficient and Sodium Concentration Measurements in Human Prostate Tissue via Hydrogen-1 and Sodium-23 Magnetic Resonance Imaging in a Clinical Setting at 3 T. Investigative radiology. 2012.
36 Rosen Y, Lenkinski RE. Sodium MRI of a human transplanted kidney. Acad Radiol. 2009;16(7):886-9.
37 Haneder S, Michaely HJ, Schoenberg SO, et al. Assessment of renal function after conformal radiotherapy and intensity-modulated radiotherapy by functional (1)H-MRI and (23)Na-MRI. Strahlenther Onkol. 2012;188(12):1146-54.
38 Trattnig S, Welsch GH, Juras V, et al. 23Na MR imaging at 7 T after knee matrix-associated autologous chondrocyte transplantation preliminary results. Radiology. 2010;257(1):175-84.
39 Zbyn S, Stelzeneder D, Welsch GH, et al. Evaluation of native hyaline cartilage and repair tissue after two cartilage repair surgery techniques with 23Na MR imaging at 7 T: initial experience. Osteoarthritis Cartilage. 2012;20(8):837-45.
40 Juras V, Zbyn S, Pressl C, et al. Sodium MR imaging of Achilles tendinopathy at 7 T: preliminary results. Radiology. 2012;262(1):199-205.
41 Ouwerkerk R, Bleich KB, Gillen JS, Pomper MG, Bottomley PA. Tissue sodium concentration in human brain tumors as measured with 23Na MR imaging. Radiology. 2003;227(2):529-37.
42 Thulborn KR, Lu A, Atkinson IC, Damen F, Villano JL. Quantitative sodium MR imaging and sodium bioscales for the management of brain tumors. Neuroimaging Clin N Am. 2009;19(4):615-24.
43 Maudsley AA, Hilal SK. Biological aspects of sodium-23 imaging. Br Med Bull. 1984;40(2):165-6.
44 Thulborn KR, Davis D, Snyder J, Yonas H, Kassam A. Sodium MR imaging of acute and subacute stroke for assessment of tissue viability. Neuroimaging Clin N Am. 2005;15(3):639-53, xi-xii.
45 Thulborn KR, Gindin TS, Davis D, Erb P. Comprehensive MR imaging protocol for stroke management: tissue sodium concentration as a measure of tissue viability in nonhuman primate studies and in clinical studies. Radiology. 1999;213(1):156-66.
46 Zaaraoui W, Konstandin S, Audoin B, et al. Distribution of brain sodium accumulation correlates with disability in multiple sclerosis: a cross-sectional 23Na MR imaging study. Radiology. 2012;264(3):859-67.
47 Rochitte CE, Kim RJ, Hillenbrand HB, Chen EL, Lima JA. Microvascular integrity and the time course of myocardial sodium accumulation after acute infarction. Circ Res. 2000;87(8):648-55.
48 Ouwerkerk R, Bottomley PA, Solaiyappan M, et al. Tissue sodium concentration in myocardial infarction in humans: a quantitative 23Na MR imaging study. Radiology. 2008;248(1):88-96.
49 Sandstede JJ, Hillenbrand H, Beer M, et al. Time course of 23Na signal intensity after myocardial infarction in humans. Magn Reson Med. 2004;52(3):545-51.
50 Laymon CM, Oborski MJ, Lee VK, et al. Combined imaging biomarkers for therapy evaluation in glioblastoma multiforme: correlating sodium MRI and F-18 FLT PET on a voxel-wise basis. Magn Reson Imaging. 2012;30(9):1268-78.
51 Kline RP, Wu EX, Petrylak DP, et al. Rapid in vivo monitoring of chemotherapeutic response using weighted sodium magnetic resonance imaging. Clin Cancer Res. 2000;6(6):2146-56.
52 Babsky AM, Hekmatyar SK, Zhang H, Solomon JL, Bansal N. Application of 23Na MRI to monitor chemotherapeutic response in RIF-1 tumors. Neoplasia. 2005;7(7):658-66.
53 Sharma R, Kline RP, Wu EX, Katz JK. Rapid in vivo Taxotere quantitative chemosensitivity response by 4.23 Tesla sodium MRI and histo-immunostaining features in N-Methyl-N-Nitrosourea induced breast tumors in rats. Cancer Cell Int. 2005;5:26.
54 Schepkin VD, Chenevert TL, Kuszpit K, et al. Sodium and proton diffusion MRI as biomarkers for early therapeutic response in subcutaneous tumors. Magn Reson Imaging. 2006;24(3):273-8.
55 Schepkin VD, Lee KC, Kuszpit K, et al. Proton and sodium MRI assessment of emerging tumor chemotherapeutic resistance. NMR Biomed. 2006;19(8):1035-42.
56 Henzler T, Konstandin S, Schmid-Bindert G, et al. Imaging of tumor viability in lung cancer: initial results using 23Na-MRI. Rofo. 2012;184(4):340-4.
57 Gerlinger M, Rowan AJ, Horswell S, et al. Intratumor heterogeneity and branched evolution revealed by multiregion sequencing. N Engl J Med. 2012;366(10):883-92.
58 Kuntz J, Gupta R, Schonberg SO, Semmler W, Kachelriess M, Bartling S. Real-time X-ray-based 4D image guidance of minimally invasive interventions. European radiology. 2013.
59 Schonberg SO, Wangler B. From molecular imaging markers to personalized image-guided therapy. Zeitschrift fur medizinische Physik. 2013.

Contact
Stefan Haneder, M.D.
Institute of Clinical Radiology
and Nuclear Medicine
University Medical Center Mannheim
Heidelberg University
Theodor-Kutzer-Ufer 1–3
68167 Mannheim
Germany
Phone: +49/621/383 2067
Fax: +49/621/383 1910
stefan.haneder@umm.de